PAPER

How many phases nucleate in the bidimensional Potts model?

Journal of Statistical Mechanics: Theory and Experiment
An IOP and SISSA journal

PAPER: Classical statistical mechanics, equilibrium and non-equilibrium

How many phases nucleate in the bidimensional Potts model?

Federico Corberi[1], Leticia F Cugliandolo[2,3], Marco Esposito[4,*], Onofrio Mazzarisi[1,5] and Marco Picco[2]

[1] Dipartimento di Fisica E. R. Caianiello and INFN, Gruppo Collegato di Salerno, Università di Salerno, via Giovanni Paolo II 132, 84084 Fisciano (SA), Italy
[2] Sorbonne Université, CNRS UMR 7589, Laboratoire de Physique Théorique et Hautes Energies, 4 Place Jussieu, 75252 Paris Cedex 05, France
[3] Institut Universitaire de France, 1, rue Descartes, 75231 Paris Cedex 05, France
[4] Imperial College London, Chain Building, 7 Imperial College Rd, Kensington, London, SW7 2AZ, United Kingdom
[5] Max Planck Institute for Mathematics in the Sciences, Inselstraβe 22, 04103 Leipzig Germany
E-mail: m.esposito18@imperial.ac.uk

Received 3 February 2022
Accepted for publication 17 June 2022
Published 20 July 2022

Online at stacks.iop.org/JSTAT/2022/073204
https://doi.org/10.1088/1742-5468/ac7aa9

Abstract. We study the kinetics of the two-dimensional $q > 4$-state Potts model after a shallow quench to a temperature slightly below the critical one and above the pseudo spinodal. We use numerical methods and we focus on intermediate values of q, $4 < q \leqslant 100$. We show that, initially, the system evolves as if it were quenched to the critical temperature: the configurations exhibit correlations that are indistinguishable from the ones in equilibrium at $T_c(q)$ over longer and longer length scales as time elapses. The further decay from the metastable state occurs by nucleation of an average number k out of the q possible phases. For a given quench temperature, k is a logarithmically increasing function of the system size, bounded by q. This unusual finite size dependence is a consequence of a scaling property underlying the nucleation phenomenon for these parameters.

*Author to whom any correspondence should be addressed.

1742-5468/22/073204+19$33.00

Keywords: classical Monte Carlo simulations, classical phase transitions, metastable states, nucleation

Contents

1. Introduction

When a control parameter is changed across a first-order phase transition one observes hysteresis and metastability. These phenomena are widespread in nature [1] and, particularly, in many areas of physics [1–5]. Besides, metastability plays a prominent role also in biological systems such as, for instance, proteins and nucleic acids [6, 7].

The simplest example of metastability is provided by a uniaxial ferromagnet in an external field, whose paradigmatic modelisation is the Ising model. Upon field reversal, on condition that its magnitude is sufficiently small and the temperature is subcritical, the magnetisation remains at the pre-reversal value for a certain time, the lifetime of the metastable state, before flipping to the new equilibrium value. The phenomenon can be ascribed to the competition between surface tension and bulk energy and is accounted for, at least at a simple semi-quantitative level, by classical nucleation theory [1, 8–10]: a *nucleus* of the equilibrium phase in a metastable sea is unstable unless its size exceeds a critical value. As long as the nucleus remains subcritical it is more likely to shrink and disappear than to grow, but as soon as it has exceeded the critical size it will keep growing with larger probability than that for shrinking. Then, in this picture, the lifetime of the metastable state is the time needed to nucleate, by thermal fluctuations, critical nuclei (notice that in this context *critical* does not refer to the criticality of the state at T_c), and to grow them until magnetisation is reversed. Elaborating on these ideas, more refined theories of nucleation [11–22] have been developed, and they describe the phenomenon with good accuracy.

In the previous example, the metastable and equilibrium states are associated to the two ergodic components which characterise the zero field infinite system at low temperatures. However, the situation is not as well understood in systems with more than two ergodic components, such as those described at the simplest level by the ferromagnetic

J. Stat. Mech. (2022) 073204

Potts model [23]. This model is defined in terms of lattice discrete variables taking $q \geqslant 2$ possible values, sometimes called colours, and the interaction favours equal colour on nearest neighbour sites. For $q = 2$, the Ising model is recovered.

In the absence of external fields, the Potts model undergoes a phase transition between a high temperature disordered phase and a low temperature, spontaneously symmetry broken, ordered one at a q-dependent critical temperature $T_c(q)$. In two dimensions, the character of the transition changes at $q = 4$ [24, 25]: for $q \leqslant 4$ it is continuous (second-order), while for $q > 4$ it is discontinuous (first-order) and metastability is found. Specifically, upon quenching from $T > T_c$ to $T \lesssim T_c$ a finite-size system remains disordered for some time, before starting the evolution towards the final equilibrium which amounts to one of the q symmetry related low-temperature ordered states. Hence, at variance with the field-driven transition in the Ising model, in the $q > 4$ cases nucleation of multiple phases occurs, and one speaks of *multi-nucleation*. Another important difference is that one has a first-order transition that is temperature driven.

The determination of the lifetime of the metastable state, its dependence on the system size, the dynamic escape from it, and the nature of the nucleation process are difficult and much debated issues [26–29, 32]. In particular, it was argued [30, 31, 33] that both the lifetime of the metastable state and the temperature range below T_c where metastability may exist in the Potts model, shrink when the system size increases. This poses yet unresolved questions on the nature of the metastable state in the thermodynamic limit.

In a previous paper [34], some of us addressed some aspects of this problem analytically with a perturbation scheme valid for large q. It turns out that, for $q \to \infty$, a long lived metastable state exists for quenches to final temperatures T which are larger than T_ℓ, where $T_\ell \to T_c/2$ in this large q limit. In [34] a rather precise description of the metastable state was given, both from the microscopic and thermodynamic points of view. However, a similar characterisation of the escape kinetics is still missing for finite q. Specifically, while the nature of the metastable state can be well described in such an analytical framework, its lifetime (for finite q) has not been determined yet and its very existence in the thermodynamic limit could not be proved. Related to this issue, the order in which the two limits of large q and large system size are taken should be specified and considered.

In this paper we study the process whereby the disordered metastable state is run away and the way in which the target equilibrium state is approached in the square lattice Potts model with $q > 4$, after shallow quenches from high to low temperatures close to T_c. We use Monte Carlo numerical simulations with the Metropolis rule for different values of q and linear system sizes L. We choose q values which are larger than 4, $q = 9, 24, 100$, but not too large so that we can observe nucleation in a relatively wide temperature interval below T_c, see [34]. In a companion paper by some of us [35] the related issue of deep quenches below the pseudo-spinodal of the same model for much larger q values, closer to the ideal $q \to \infty$ limit, is tackled and the full parameter dependence of the curvature-driven growing length in the coarsening regime is determined.

Our main result is the characterisation of the multi-nucleation process. We show that,

J. Stat. Mech. (2022) 073204

- For a restricted time after the quench, the system evolves as if it were at the critical temperature or slightly above it.
- Later, multi-nucleation takes over. We argue that for a given system size, the number k of phases that nucleate is a logarithmically increasing function of L,

$$k \propto \ln L \quad \text{for } 4 < q \leqslant 100, \tag{1}$$

with $k \leqslant q$, see equation (16).

In addition, we also study the dependence of k on q and T. After the metastable state is escaped, colours which do not nucleate remain in the system only in the form of thermal fluctuations. Those which nucleate start competing, resulting in a coarsening process [35–46] which leads, at some point, to a single dominating phase and equilibrium is attained (at not too low temperatures; otherwise, blocked states of the kind discussed in [35–40] can be attained).

The paper is organised as follows. In section 2, we introduce the Potts model and its dynamics. We also define the relevant observables that will be further considered. In section 3, we provide a general description of the whole dynamical process, from the instant of the quench, to the escape from metastability and further on. Section 4 is the core of the article and contains a thorough discussion of the multi-nucleation process. Finally, section 5 concludes the paper.

2. Model and observables

The Hamiltonian of the Potts model [23] reads

$$H[\{s_i\}] = -J\sum_{\langle ij\rangle}\delta_{s_i s_j}, \tag{2}$$

where $J > 0$ is a coupling constant and $\langle ij\rangle$ are nearest-neighbour couples on a two-dimensional square lattice of linear dimension L. δ_{ab} is the Kronecker delta and s_i is an integer variable ranging from 1 to $q \geqslant 2$. We consider periodic boundary conditions. In the sum we count each bond once, and for this geometry the energy is bounded between $-2JL^2$ and 0. The critical temperature is exactly known in $d = 2$ [23]

$$k_{\mathrm{B}}T_{\mathrm{c}}(q) = \frac{J}{\ln\left(1+\sqrt{q}\right)} \tag{3}$$

and the phase transition is second- (first-) order for $q \leqslant 4 (q > 4)$ [47]. Notice that for finite systems of size L, denoting with $T_{\mathrm{c}}(L, q)$ the finite size critical temperature, the corrections to the infinite size $T_{\mathrm{c}}(q)$ given in equation (3) go as $(T_{\mathrm{c}}(L, q) - T_{\mathrm{c}}(q))/T_{\mathrm{c}}(q) \simeq L^{-d}$ [48]. Henceforth we will set $k_{\mathrm{B}} = J = 1$.

We consider the dynamics where single spins are updated according to a random sequence with a probability $w(s, s')$ to change from an initial value s to a final one s'. We use the Metropolis form $w(s, s') = \min[1, \exp(-\Delta E/T)]$, where ΔE is the energy

J. Stat. Mech. (2022) 073204

variation associated to the flip. A unit time, or Monte Carlo step, is elapsed after L^2 attempted moves.

In the following we will consider a protocol in which the system, initially prepared in an infinite temperature equilibrium state, is suddenly quenched at time $t = 0$ to a low temperature $T < T_c$. The dynamical evolution has been studied in previous works [35–46] mainly focussing on the coarsening regime. Here we are interested in metastability and multi-nucleation, which clearly arise at $T \lesssim T_c$.

After the quench the system relaxes to a low energy state and the energy density $e(t) = \langle H[\{s_i\}](t)\rangle/L^2$ approaches the final equilibrium value $e(\infty)$. Here and in the following the non equilibrium average $\langle\cdots\rangle$ is taken over thermal histories and initial conditions. In order to quantify the relaxation we will consider the energy density excess

$$\Delta e(t) = e(t) - e(\infty). \tag{4}$$

In a configuration with well formed domains, connected regions with the same spin state, the excess energy is stored on the domain walls, and $\Delta e(t)$ is proportional to the density of interfacial spins. Since for non fractal aggregates this quantity is, in turn, inversely proportional to the typical size of the domains, from $\Delta e(t)$ one can infer such characteristic length as

$$R(t) = \Delta e(t)^{-1}. \tag{5}$$

This definition becomes questionable for instance in the initial stages of the process when domains are not formed. Therefore we will discuss below another determination of a typical length scale based on the measurement of spatial correlations.

A fundamental quantity, usually considered in coarsening processes, is the equal time spin–spin correlation function. Specifically, we define the quantity

$$C_{ij}(r,t) = \left.\frac{\sum_{n=1}^{q}\left[\langle\delta_{s_i(t),n}\delta_{s_j(t),n}\rangle - \langle\delta_{s_i(t),n}\rangle\langle\delta_{s_j(t),n}\rangle\right]}{\left(\sum_{n=1}^{q}\left[\langle\delta^2_{s_i(t),n}\rangle - \langle\delta_{s_i(t),n}\rangle^2\right]\right)^{1/2}\left(\sum_{n=1}^{q}\left[\langle\delta^2_{s_j(t),n}\rangle - \langle\delta_{s_j(t),n}\rangle^2\right]\right)^{1/2}}\right|_{|\vec{r}_i-\vec{r}_j|=r}. \tag{6}$$

In order to obscure the effects of the lattice anisotropy, we will only consider couples i, j along the horizontal and vertical directions. In this case, due to invariance under rotation over 90 degrees and homogeneity, $C_{ij}(r,t)$ only depends on the distance $r = |\vec{r}_i - \vec{r}_j|$, where $\vec{r}$ is the vector joining i and j, and for given r should be independent of i or j. Hence, further on we will denote it as $C(r,t)$ and, enforcing this symmetry, we will rather compute the spatial average of the quantity in equation (6), namely $L^{-2}\sum_{ij} C_{ij}(r,t)$, where i runs over all the lattice and j only over sites at distance r (in horizontal or vertical direction) from i. In this way, we will improve the statistics. Labelling of the q possible values of the spins will be done in the following in a dynamical way: at any time we order the colours according to their abundances, from the most to the least represented, and label them with n increasing from 1 to q. This method is useful, particularly in the late stage of the dynamics where, as we will discuss, a clear hierarchy of abundances sets in. We have checked that some exchanges in the ordering occur during evolution for the q values we use here but these are rare. Roughly speaking, a

J. Stat. Mech. (2022) 073204

hierarchy of colours is installed by the sequence in which the phases nucleate. Defining

$$\sigma_n^2(t) = \langle \delta_{s_i(t),n}^2 \rangle - \langle \delta_{s_i(t),n} \rangle^2. \tag{7}$$

Equation (6) can be rewritten as

$$C(r,t) = \frac{\sum_{n=1}^{q} \sigma_n^2(t) C_n(r,t)}{\sum_{n=1}^{q} \sigma_n^2(t)}, \tag{8}$$

where

$$C_n(r,t) = \frac{\langle \delta_{s_i(t),n} \delta_{s_{i+\vec{r}}(t),n} \rangle - \langle \delta_{s_i(t),n} \rangle \langle \delta_{s_{i+\vec{r}}(t),n} \rangle}{\sigma_n^2(t)} \tag{9}$$

is the correlation function restricted to the colour n. Equation (8) transparently expresses the fact that the unrestricted correlation is the weighted average of the restricted ones, the weights being the variances associated to s_i by equation (7).

Dynamical scaling holds if $C(r,t)$ takes the form

$$C(r,t) \sim g\left[\frac{r}{\mathcal{R}(t)}\right], \tag{10}$$

for $r \gg a$ a microscopic length scale, where g is a scaling function and $\mathcal{R}(t)$ a characteristic size with the meaning of the typical domain's linear dimension. From the correlation function one can extract such a size in different ways. For instance, one can use the moments as

$$\mathcal{R}(t) = \mathcal{R}_\mu(t) = \left[\frac{\sum_r r^\mu C(r,t)}{\sum_r C(r,t)}\right]^{\frac{1}{\mu}}. \tag{11}$$

In case of dynamical scaling, determinations with different values of μ provide proportional results (however large μ values are numerically problematic since the noisy large-r tails of $C(r,t)$ are heavily weighted). Similarly, one can use the half-height width to define $\mathcal{R}(t)$ through

$$C(\mathcal{R}(t),t) = \frac{1}{2}. \tag{12}$$

In the following we will use this determination which is easier to implement. Analogously, the typical size of the domains of a specific colour $\mathcal{R}_n(t)$ can be defined replacing C with C_n in equation (12):

$$C_n(\mathcal{R}_n(t),t) = \frac{1}{2}. \tag{13}$$

Let us mention that equation (13) cannot be used to determine the domain size of colour n in two situations: (i) the corresponding colour is not present in the system (apart from thermal fluctuations). In this case $C_n \simeq 0$, equation (13) loses its meaning, and $\mathcal{R}_n$ could be taken to be zero. (ii) The colour has invaded the whole system.

J. Stat. Mech. (2022) 073204

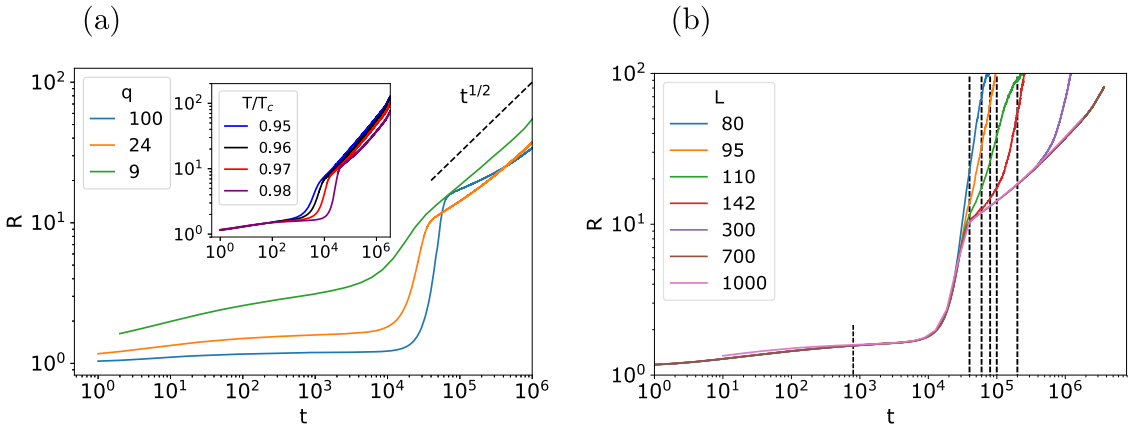

Figure 1. (a) The time evolution of the growing length R defined in equation (5) for $q = 9, 24, 100$ (see the key). The linear system size is $L = 700$. The dashed segment shows the asymptotic curvature driven growth $t^{1/2}$. In the inset the T/T_c dependence of R in the case $q = 24$ and $L = 700$ is shown. (b) $R(t)$ for $q = 24$ and different linear system sizes $L = 80, 95, 110, 142, 300, 700, 1000$ (the last two curves superimpose). The dashed vertical segments indicate the times at which the snapshots of figure 2 were taken. The time dependence is discussed in the text.

In this case C_n decays to zero on a distance of the order of the size of thermal fluctuations (note that C is a connected correlation) and is not related to the size of the domain of the winning colour which is close to the system size L. In general, immediately before one of the two situations (i) or (ii) occurs, one measures a very small value of $\mathcal{R}_n$. Hence it must be kept in mind that a small value of $\mathcal{R}_n$ does not necessarily mean that the corresponding colour is present only in small domains, but it could as well be that it has flooded the system. Which case applies must be ascertained differently, for instance, by visual inspection of the configurations. This will be important further on.

3. The dynamical process

In the following we will discuss the results of the numerical simulations of the Potts model introduced in equation (2). We will mainly consider three q values, $q = 9$, 24, 100, as paradigms of small, intermediate and large q behaviour. Other q values have also been studied and we sometimes include them in the presentation. These systems are quenched to final temperatures close to the critical ones, $T_c(q)$, in order to investigate the metastable state and its lifetime. In most of our simulations we set $T = 0.9912 \cdot T_c(q)$ for $q = 9$, $T = 0.98 \cdot T_c(q)$ for $q = 24$, and $T = 0.95 \cdot T_c(q)$ for $q = 100$. These choices are motivated by the requirement to have a comparable nucleation time $\tau(q, T)$ (see discussion below, and figure 1) for the three reference values of q. Notice that fixing $\tau(q, T)$ does not mean that, for different q, one has the same value of $(T_c(q) - T)/T_c(q)$. Let us also remind that, as discussed below equation (3), $T_c(q)$ is the critical temperature of the infinite system. In order to investigate the finite-size effects, a central issue of this

J. Stat. Mech. (2022) 073204

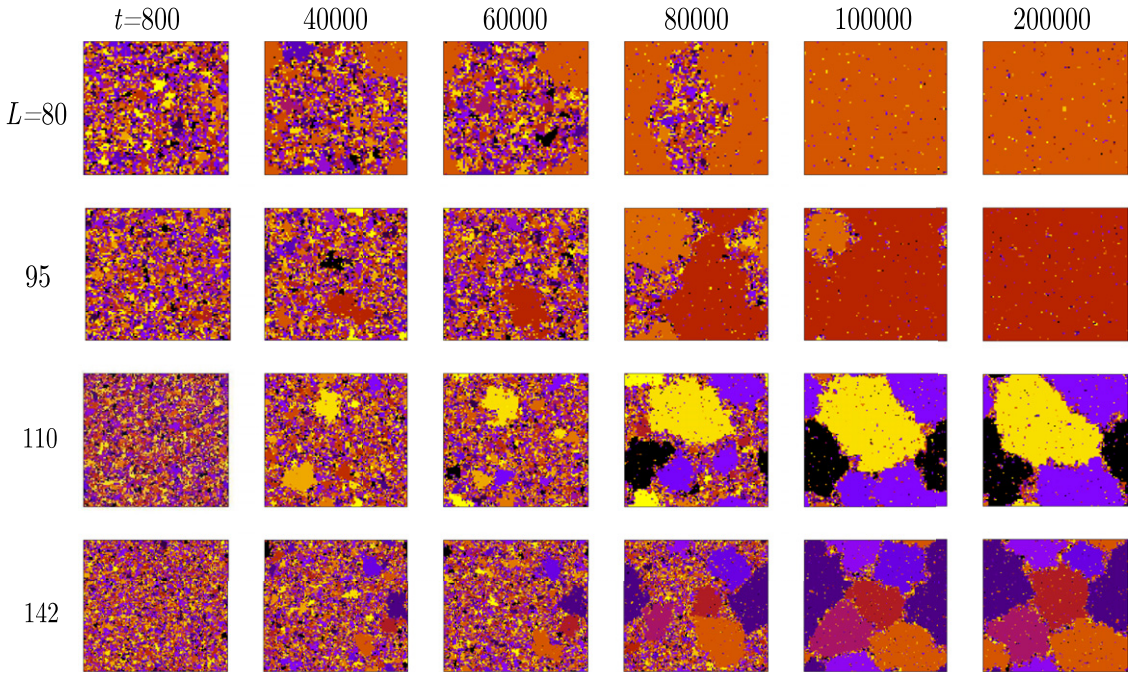

Figure 2. Snapshots of a typical evolution of the $q = 24$ Potts model quenched to $T = 0.98 \cdot T_c$ for different lattice sizes. It is possible to appreciate that the number of phases that nucleate increases with the linear size of the system: $k = 1$ for $L = 80$, $k = 2$ for $L = 95$, $k = 3$ for $L = 110$ and $k = 6$ for $L = 142$, all at $t = 10^5$.

paper, we will use systems in the range of sizes $L \in [200, 1000]$ (only for qualitative illustrations, such as the snapshots in figure 2, we consider systems as small as $L = 80$). Comparing the value of the equilibrium coherence length ξ at $T_c^+(q)$ given in [49] with the system sizes we use, one concludes that L/ξ is at least 13 (in the worst case $L = 200$ with $q = 9$). Therefore our studies are expected to be basically free from the usual equilibrium finite size effects occurring when L is smaller than or comparable to ξ. Concerning finite size effects in the non equilibrium process, one has to control that, at least, the size of the domains present in the system is much smaller than L. For these reasons the quantitative analysis performed below does not go beyond the time $t = 10^7$, namely, when such finite size effects start appearing for the largest, $L = 10^3$, system considered. In figure 1(b) this corresponds to the time when, in a system of size L, we see a second jump of R (e.g. for $L = 300$, starting around $t = 6 \cdot 10^5$), linked to the fact that only just a few domains remain. This, however, does not exclude other finite size effects of non-equilibrium nature, which are indeed a central point of this article, as we will explain below.

A first qualitative description of the kinetic process after the quench stems from the behaviour of $R(t)$, the typical length scale extracted from the analysis of the excess energy as in equation (5), which is shown in figure 1. With some quantitative differences, the same kind of pattern is observed for any value of q (see also [37, 44, 50] where this quantity, for more T and q values, respectively, was shown). After a short transient, one can clearly identify three extended regimes. The first one is associated to R growing

J. Stat. Mech. (2022) 073204

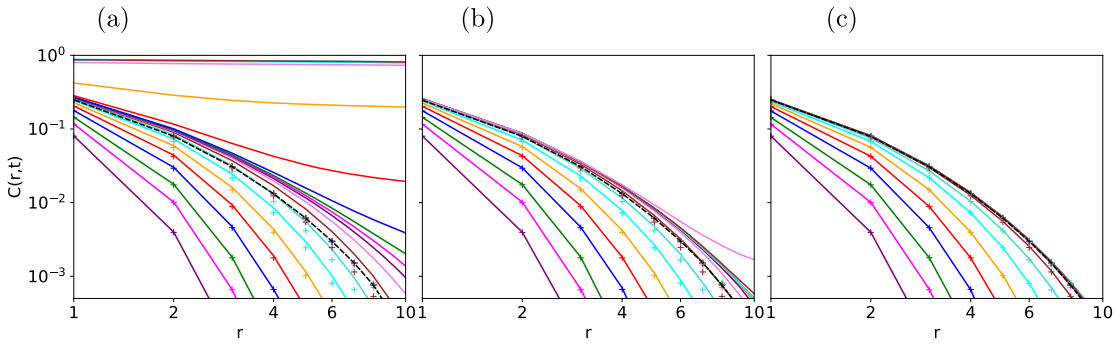

Figure 3. The space–time correlation function $C(r,t)$ is plotted with continuous lines against r for a quench of the model with $q = 24$ and $L = 700$, from infinite temperature to $T = 0.99 \cdot T_c$ (a), $T = 0.995 \cdot T_c$ (b), $T = 0.999 \cdot T_c$ (c). Different curves correspond to different times exponentially spaced (from bottom to top $t = 2, 4, 7, 15, 31, 64, 137, 291, 618, 1316, 2802, 5968, 12\,709, 27\,066, 57\,642, 122\,762, 261\,451, 556\,822, 1185\,886$). The crosses refer to a quench to $T = T_c$ and the black dashed lines represent the final equilibrium state. See the text for a discussion.

slowly or staying approximately constant, $R(t) \simeq R_m$. This plateau, which is flatter and longer as $T \to T_c^-$ at fixed q or as $q \to \infty$ at fixed $(T - T_c)/T_c$, is a clear manifestation of metastability. In this time lag the kinetics is slow and for sufficiently large q has almost no effect because the system is confined in a local free energy minimum and the trapping barrier is not yet jumped over. In order to do it, critical nuclei, namely ordered domains of a sufficiently large size, must develop. However, this is an activated process which requires a certain time $\tau(q,T)$, the nucleation time. At $t \ll \tau(q,T)$ the system is still in a rather disordered state, visually not too different from the initial one, see the snapshots taken at $t = 800$ in figure 2. Some small ordered domains can be spotted but they are too tiny to start nucleation.

Actually, this metastable state is *similar* to the equilibrium one at T_c, in a sense that we are going to specify below. We illustrate this point by means of the correlation function defined in equation (6). In figure 3 this quantity is plotted against r during the evolution after a quench. Let us focus, to start with, on figure 3(a), where curves for a quench to $T = 0.99 \cdot T_c$ (continuous lines) are compared to those, taken at the same times, for a quench to $T = T_c$ (crosses). In the latter case one sees that, as time goes on, the correlation extends to larger values of r until at $t \simeq t_{eq}(T_c) \simeq 10^3$ the curves start to superimpose, signalling that equilibrium has been reached (dashed ones). Notice that, according to the results in [49], the equilibrium coherence length at T_c is $\xi = 2.1554$ for the case with $q = 24$ considered here. Hence the range of distances plotted in figure 3 extends well beyond ξ. At short times, a similar pattern is displayed by the curves of the subcritical quench (continuous ones) which stay close to the ones previously discussed. At longer times, for $t > t_{eq}(T_c)$, the correlations move to the right further than those of the quench to T_c and there is tendency to accumulate on a curve somewhat broader than the equilibrium one at T_c. This occurs roughly in the range of times $t \in [10^3, 10^4]$ which corresponds to the nucleation time. In this time range the correlation is almost time-independent at short r, whereas some evolution can be spotted at large r. This

J. Stat. Mech. (2022) 073204

signals that the metastable state is not really stable, and that a prodrome of its decay, which can be interpreted as the build up of supercritical nuclei, is becoming manifest at large distances. Finally, roughly for $t > 10^4$, a quick growth of correlations is observed, unveiling that metastability is over and that the next stage, where ordering takes place, has been entered. In this case, the classification of the behaviour of the correlation into three stages (initial evolution, stasis, late evolution) is not sharp because, as we discuss below, T is relatively far from T_c.

Let us now have a look at the other two panels in figure 3. In the central one (b) the quench is closer to T_c and the accumulation of curves in the metastable state is clearer than in the left panel. Furthermore, the locus where superposition occurs is also closer to the equilibrium curve at T_c than in the left panel. In the right panel (c) the subcritical quench is so close to T_c that the departure from the metastable state cannot even be measured within the simulated times. Besides that, one sees a pattern similar to the one observed in the other panels, with the notable difference that the correlations in the metastable state are almost indistinguishable from the ones of a system relaxing to equilibrium at T_c. This clarifies our statement that the metastable state is *similar* to the equilibrium one at T_c: the closer to T_c the quench is, the longer the life-time of the metastable state and the more similar to equilibrium at T_c it is[6].

The nucleation time $\tau(q, T)$ can be roughly identified as the time when the plateau is over and R jumps rather abruptly to a higher value, see figure 1. This is a violent process corresponding to the fast invasion of available space by the super-critical nuclei, as it can be seen from the snapshots in figure 2 corresponding to $t = 4 \cdot 10^4$ and $t = 6 \cdot 10^4$. Such speedy relaxation becomes sharper upon increasing q.

The duration $\tau(q, T)$ of the metastable state increases as $T \to T_c^-$, as it can be seen in the inset of figure 1(a). In the same picture we can also observe that the plateau value R_m is rather T-independent while, instead, there is a clear dependence on q. In [50] it was found that this value is well approximated by $R_m \propto [\ln(q-4)]^{-1}$ for small q ($q \lesssim 50$) and then, increasing further q, it saturates to a value of order one. This dependence can be understood recalling that R_m is the inverse energy density excess (equation (5)). The energy density e_m in the metastable state was computed in [34] and goes to zero for large q as $e_m \simeq -a(T)q^{-1/2}$, where $a(T) > 0$ is a temperature dependent factor. On the other hand, the asymptotic equilibrium quantity $e(\infty) < 0$ becomes independent of q [52] for large q. Therefore, we conclude that $\Delta e_m = e_m - e(\infty)$ approaches a large-q value ($-e(\infty)$) from below, as observed. Given the choice of temperatures made in figure 1(a) (so as to have roughly $\tau(q, T)$ fixed) it is clear that, changing q and working instead at a constant T or even at a finite fraction of $T_c(q)$, i.e. $T = x \cdot T_c(q)$, the lifetime of metastability increases with q. Similarly, we have also noticed that the temperature range with metastability widens for larger q. Specifically, indicating with T_ℓ the lower temperature where metastability is still observed we find that $(T_c - T_\ell)/T_c$ increases with q.

[6] Note that this is quite different from what happens in the paradigmatic example of nucleation: the Ising model, at constant $T < T_c$, under a reversing field. In this case, and in the typical Ginzburg–Landau double-well representation, it is claimed that the system globally remains in the ordered metastable state after reversing the field, with no long-range effect of the post-quench field, until the critical radius is reached, and the new equilibrium configuration invades the full system. Of course the nucleation process leading to equilibration is similar.

J. Stat. Mech. (2022) 073204

The fast process associated to the steep increase of R ends at a time $t_{\rm coal}$ when $\mathrm{d}^2R/\mathrm{d}t^2$ becomes negative. (Notice that this definition is meaningful for sufficiently large sizes L, say $L > 110$, as it can be seen in figure 1(b). For such sizes this occurs around $t = 4 \cdot 10^4$. For smaller sizes $\mathrm{d}^2R/\mathrm{d}t^2$ may not show the change of sign as finite size effects produce a faster growth of R due to the prevailing presence of the winning colour.) Looking at figure 2, one sees that this time roughly corresponds to configurations where nuclei of different colour start to come in contact. At this point a coarsening phenomenon sets in produced by the competition among domains, as shown in figure 2 and reported in [36–38, 41–46] and, for the closely related *vector Potts* (or clock) model, in [51]. In this kind of evolution one has phase ordering kinetics and expects dynamical scaling with $R(t) \sim t^{1/2}$, which is indeed roughly noted in figure 1 at very long times (for $q = 100$ this behaviour is likely to be reached at times longer than the simulated ones). Since this regime is not the focus of this paper we content ourselves with such a semi-quantitative indication.

Before closing this section let us comment on the fact that the data for R are free from finite-size effects until domains coarsen up to a length comparable to the system size, which occurs at a time $t_{\rm fs}(L)$ that can be recognised as the time when the curve for $R(t)$ for a given L departs from the corresponding one for $L = \infty$. This can be seen in figure 1(b) where one sees that the curves deviate from the one corresponding to the larger system size ($L = 1000$) when $R(t) \simeq 0.1 \cdot L$. For instance, this occurs at a time $t_{\rm fs}(L = 300)$ of order $6 \cdot 10^5$, and around $t_{\rm fs}(L = 142) \simeq 6 \cdot 10^4$. However, the fact that this particular quantity (R) does not feel the size of the system before $t_{\rm fs}(L)$ does not mean that the dynamics is globally free from finite-size effects in this time domain. Actually, in figure 2 one clearly sees that the configurations at a given time look very different in systems of different sizes. The next section is devoted to a quantitative analysis of this effect and to the discussion of such feature.

4. Multi-nucleation

In the introduction we have briefly discussed the fact that in the thermally driven first-order transition the role of the system size is important. The reason is that $\tau(q, T)$ and the pseudo-spinodal temperature depend on the system size. In the previous section we have already anticipated that, besides this feature, also the dynamic escape from the metastable state depends significantly on the system size, as a visual inspection of figure 2, where the same quench of the $q = 24$ model is operated on systems of different sizes, clearly displays. Specifically, when a relatively small size is considered ($L = 80$, upper row) a single critical droplet forms and grows, invading the whole system (last two snapshots). Basically in this case the growth time is small compared to the nucleation time (the latter is initially expected to scale as L^{-2}). This is what we call mono-nucleation, or one-nucleation. We have checked that such phenomenon is observed rather independently of the thermal realisation of the process.

In the second row the behaviour of a slightly larger system ($L = 95$) is shown. This small size increase is sufficient to qualitatively modify the situation, in that there are

J. Stat. Mech. (2022) 073204

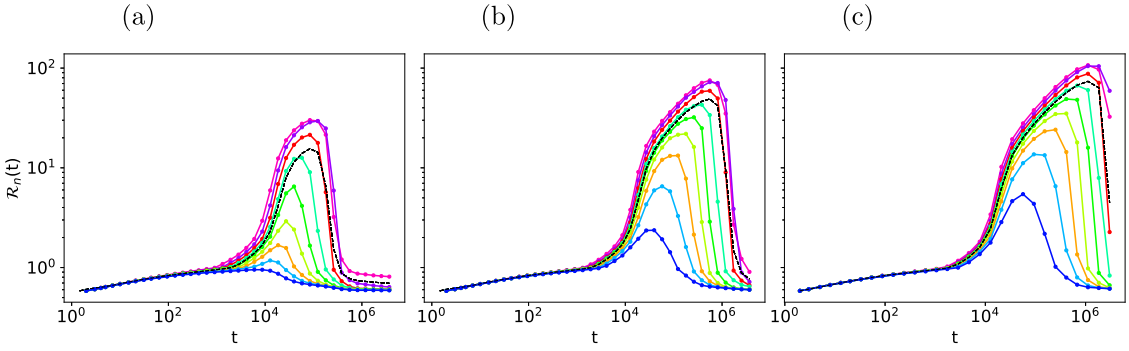

Figure 4. The typical lengths $\mathcal{R}_n$ of the various colours defined in equation (13) are plotted against time for the model with $q = 9$ quenched to $T = 0.9912 \cdot T_c$. The log–log scale is the same in the three panels. The black dashed line is the average $\mathcal{R}$. The system sizes are $L = 300$ (a), $L = 700$ (b) and $L = 1000$ (c). Each curve represents an average over 500 non-equilibrium realisations.

now two nucleating colours, the orange and the brick red ones. Then, in this case, we have bi-nucleation, or two-nucleation. Again, this feature is rather independent of the thermal realisation, as it will be shown below by means of a statistical analysis. After nucleation, surface tension closes the domain of the minority colour (last snapshot), symmetry is definitely broken and equilibrium is attained.

Increasing further the system size as in the two rows below, the fate of a system changes again and one observes three-nucleation and six-nucleation. Notice that, after multi-nucleation, the competition among domains of different colours leads to a progressive reduction of their number. Increasing further L (not shown) one can observe k-nucleation with k up to q ($q = 24$ in this example).

In order to discuss the multi-nucleation process and its dependence on the system size at a more quantitative level we consider the typical lengths of the various colours, $\mathcal{R}_n(t)$, which are shown for three different system sizes in figure 4. From this figure one clearly sees that $\mathcal{R}_n$ for the various colours initially grow, up to, on average, a characteristic time t_n^* when they reach a maximum $\mathcal{R}_n^*$ and then shrink. This means that domains of the corresponding colour grow, reach a maximum size, and then collapse and disappear. For the prevailing colour (and possibly the next ones in the hierarchy also reaching domain sizes comparable to the system size itself) denoted by #1 in figure 4, the interpretation is different, since the final decrease of $\mathcal{R}_1$ must be associated to the invasion of a significant fraction of the whole space, according to what discussed in case (ii) at the end of section 2[7].

From the comparison between the three different system sizes represented in figure 4, one can make some remarks. First, it is clear that for small sizes not all colours nucleate whereas they usually do in larger systems. For instance, colour #9, represented in blue, does not show the fast increase signalling the escape from metastability for $L = 300$ and $\mathcal{R}_9$ does not go beyond $\sim$1, whereas it does grow significantly in the larger systems with $L = 700$ and $L = 1000$. This indicates that $\mathcal{R}_n$ is a quantity one can use to establish the

[7] Notice that if only two colours remain (with $n = 1, 2$) one always has $\mathcal{R}_1 \simeq \mathcal{R}_2$ due to the definition of these lengths through the correlation function.

J. Stat. Mech. (2022) 073204

average number of nucleating colours. Secondly, from figure 4 one sees that both the peak time t_n^* and the peak height $\mathcal{R}_n^*(q,T,L)$ are increased in a larger system. Exploiting these two observations we developed a method to determine the average number of nucleating phases as a function of L and q, which we now describe.

First, we measure the maximum of $\mathcal{R}_n(t;q,T,L)$ over time, which we called $\mathcal{R}_n^*(q,T,L)$, at fixed T for all $n=1,\ldots,q$ and different system sizes. The 24 curves in the inset of figure 5(b) represent $\mathcal{R}_n^*(q,T,L)$ against L in a system with $q=24$ at fixed T. The first three panels (a)–(c) refer to different values of q, and show that the data very clearly obey a scaling form

$$\mathcal{R}_n^*(q,T,L) \equiv \max_t \mathcal{R}_n(t\,;q,T,L) = f_q\left[\frac{L}{L_n(q,T)}\right], \tag{14}$$

where $L_n(q,T)$ is a fitting parameter which is plotted as a function of n for the three q values in figure 5(d). A similar pattern is found for other values of q, not reported in the figure. Notice that imposing collapse of the curves according to equation (14) only fixes $L_n(q,T)$ up to an arbitrary multiplicative constant. We fix it by asking that the steep part of $f_q(x)$ be centred at $x=1$. As we further discuss below L_n is roughly the smallest system size for which the cluster of the nth colour reaches the critical size.

The scaling function $f_q(x)$ stays small for $x \ll 1$ and it suddenly increases around $x=1$. The increase is steeper for larger q, which is presumably due also to the fact that for large q the probability of having more than one nucleus of the same colour is greatly reduced. After this increase $f_q(x)$ behaves as $f_q(x) \sim x$ for large x (see the dashed lines in figures 5(a)–(c)). This latter trend indicates that, for each colour such that the representative point lies in this sector, the maximum size of the domains is triggered linearly by the system size, as it usually happens for a finite size effect in a standard (e.g. binary) coarsening system (see also the discussion at the end of this section). Hence, we argue that points belonging to this sector of x, i.e. $x>1$, correspond to colours that, given the system size L, have nucleated. Analogously, points in the small x sector, i.e. $x<1$, where $f_q(x)$ takes an approximately constant small value, correspond to colours that did not succeed nucleating. On the basis of this, we conclude that $x>1$, namely $L > L_n(q,T)$, is the condition for the nth colour to be in the coarsening stage. In particular, one can interpret $L_2(q,T)$ as the smallest system size in order to have competition between domains of different colour.

We also observe that the small-x plateau value of $f_q(x)$ decreases with increasing q. This can be explained recalling that points laying there are representative of colours that do not nucleate, and arguing that, as such, their properties are basically those of the metastable state. The latter, in turn, is akin to the equilibrium state at T_c, see figure 3 and its discussion in section 3, whose coherence length decreases upon increasing q [49].

The plot of $L_n(q,T)$ against n in figure 5(d), displays an exponential dependence

$$L_n(q,T) = \ell(q,T)\, e^{n/\mathcal{N}(q)}. \tag{15}$$

This law describes well all the data for $q=9,24$, and the large n ($n>20$, say) region for $q=100$. The fitting parameters are $\ell(q,T)=59.43$, 82.97, 200.00 and $\mathcal{N}(q)=3.546$, 11.848, 67.568 for $q=9,24,100$ and the temperatures used in these simulations (see the beginning of section 3), respectively. Furthermore, we found an analogous behaviour for

J. Stat. Mech. (2022) 073204

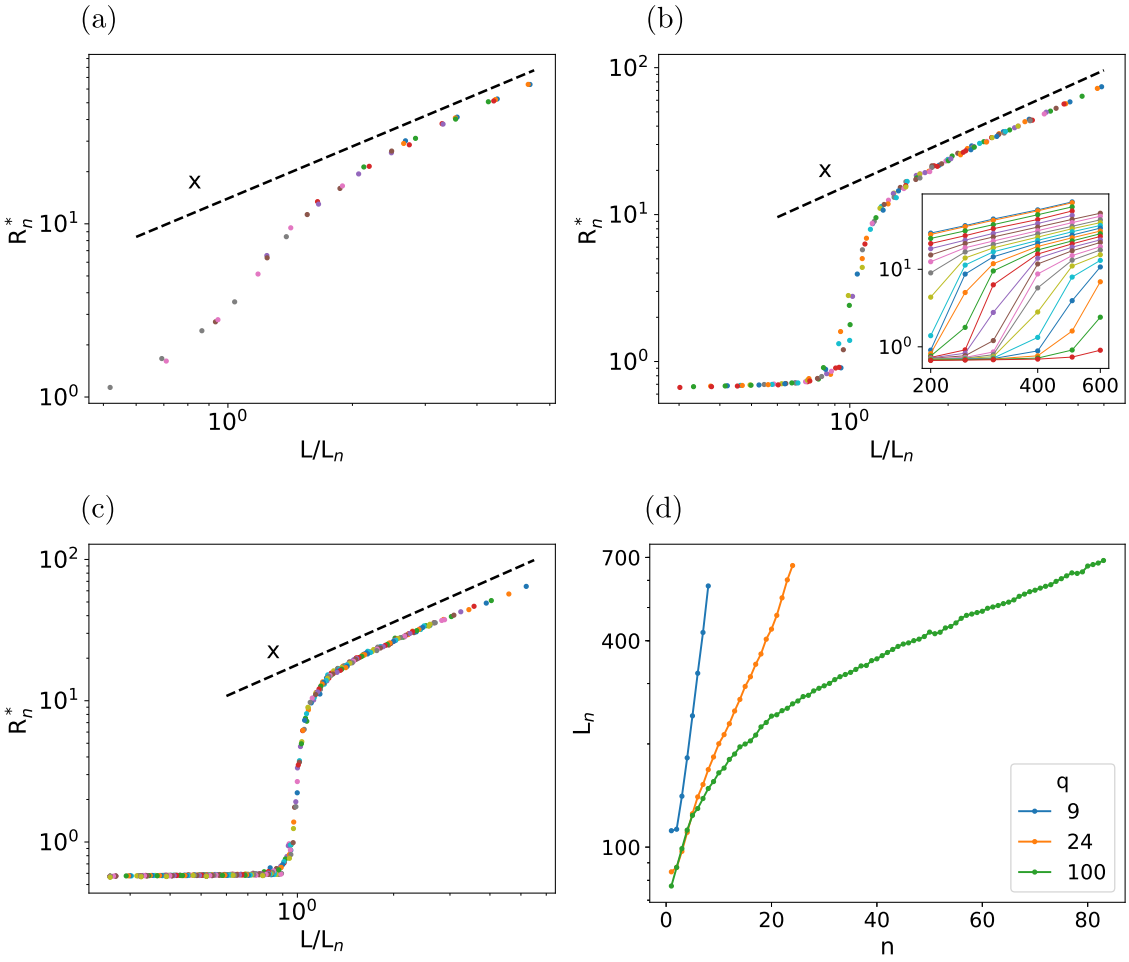

Figure 5. The maximum of $\mathcal{R}_n(t\,;q,T,L)$ over time, called $\mathcal{R}_n^*(q,T,L)$, is plotted in log–log scales against the rescaled size $x = L/L_n(q,T)$ (see the text) for $q = 9$ (a), $q = 24$ (b) and $q = 100$ (c). The system sizes are $L = 200$, $250, 300, 400, 500, 600, 700, 800$ and different colours correspond to different L data. The dashed black lines are the linear behaviour $y \sim x$. The inset in (b) contains the unscaled data ($\mathcal{R}_n^*(q,T,L)$ vs L) for $q = 24$ and various values of n (from the most abundant phase on the top, to the less abundant on the bottom). In (d) the dependence of L_n on the colour n is plotted for the three values of q, in a semi-log plot. Notice that for $q = 24$ the data in (d) are compatible with the snapshot in figure 2.

other values of q not portrayed in figure 5. Let us now discuss the q and T dependencies of the number $\mathcal{N}$ and the length scale ℓ.

Repeating the procedure above at different temperatures we find that the fitting parameter $\mathcal{N}$ is, within errors, independent of T, as shown in the inset of figure 6(a) for $q = 24$. The variation reported can be ascribed to some random effect, or errors, rather than to a genuine dependence (notice also that the fluctuations of $\mathcal{N}$ are around 10% of $\mathcal{N}$ itself). Similar results are found for other values of q. This justifies having written $\mathcal{N}(q)$, with no T dependence, in equation (15). Finally, as shown in figure 6(a), $\mathcal{N}(q)$

J. Stat. Mech. (2022) 073204

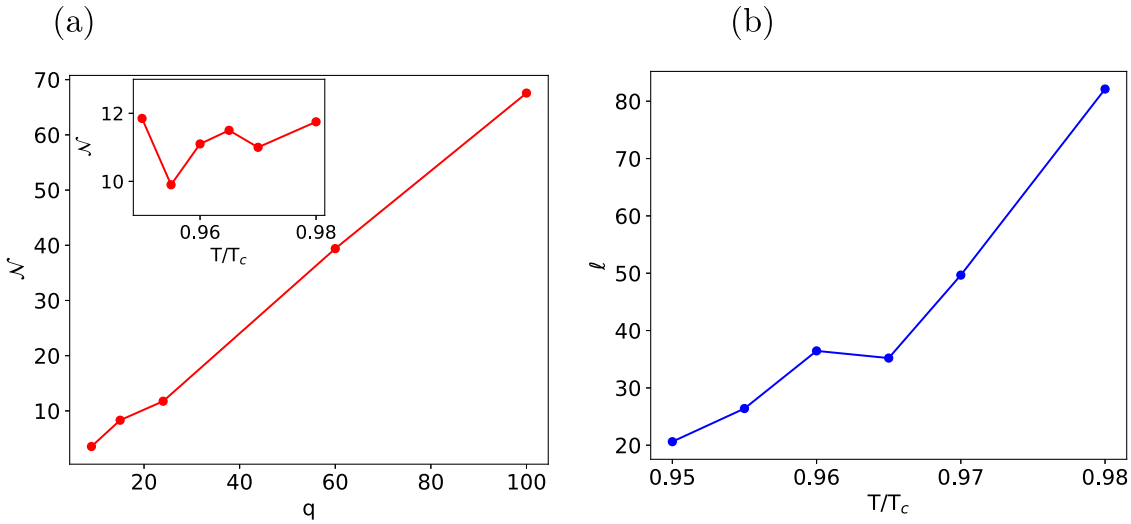

Figure 6. (a) The dependence of $\mathcal{N}$ introduced in equation (15), on q by choosing T at a q-dependent value such that the lifetime $\tau(q,T)$ of the metastable state is kept constant. In the inset the dependence of $\mathcal{N}$ on $T/T_c(q)$, for $q=24$, is displayed, showing that it is not significant (notice the narrow interval on the y-axis). (b) The dependence of ℓ, also defined in equation (15), on $T/T_c(q)$ for $q=24$.

turns out to increase in a roughly linear way with q and have a rather large range of variation.

Concerning the prefactor $\ell(q,T)$, its dependence on $T/T_c(q)$ (at fixed $q=24$) can be appreciated in the right panel of figure 6, where one finds that $\ell(q,T)$ increases with T. One could expect that $\ell(q,T)\to\infty$ for $T\to T_c$, because equation (15) would imply that all the $L_n(q,T)$ diverge in this regime, meaning that the nucleation time diverges in this limit (there is no nucleation right at T_c). The metastable state becomes the stable equilibrium one, as expected, at the critical point. On the other hand, with the choices of T made in our simulations, which as discussed earlier correspond to fixing the lifetime $\tau(q,T)$ of the metastable state, the dependence of $\ell(q,T)$ on q cannot be established and we do not show it here.

Coming to the issue of multi-nucleation, applying the argument above to $L_n(q,T)$, we can say that the nth colour, on average, may nucleate if $L>L_n$. Using equation (15) we arrive at the conclusion that, given a system size L, one has k-nucleation with

$$k(q,T,L)=\left\{\mathcal{N}(q)\ln\left[\frac{L}{\ell(q,T)}\right]\right\}_{\in[1,q]}, \tag{16}$$

where the notation $\{Z\}_{\in[1,q]}=\max\{1,\ \min\{q,Z\}\}$ simply accounts for the constraint $k\in[1,q]$ and k integer. k in the equation above has the meaning of the (average) number of colours that access the coarsening stage. One can easily check that, using the values of $\mathcal{N}(q)$ and $\ell(q,T)$ which we found fitting L_n in this equation, one can correctly predict the number of nucleating colours observed in the various cases of figure 2. Notice however that the domain of validity of this equation is inherited by the one of equation (15). Hence, if q is large it holds true only for sufficiently large values of k, see figure 5(d).

J. Stat. Mech. (2022) 073204

Moreover, as we will further discuss in section 5, we expect this logarithmic behaviour to change for values of q much larger than the intermediate ones considered in this paper.

This result shows that, for a given q, the number k of nucleating phases grows only logarithmically with the system size up to $k = q$. When the thermodynamic limit is taken from the onset, all phases nucleate.

Also, if $\ell(q, T)$ does not depend much on q, $L_n(q, T)$ decreases for increasing q (because $\mathcal{N}(q, T)$ increases). Hence increasing q increases the number of nucleating phases. This can be checked in figure 5(d). Let us also notice that equation (16) informs us on the number of nucleating phases, but does not predict the time needed to nucleate. Clearly, if this time grew towards infinity, no nucleation would be found. In the large q-limit, it was also observed that a different mechanism takes over, see for instance figures 6(c) and (d) in [35], with, possibly, a different scaling of k with L that still needs to be investigated in depth.

The discussion above shows that the multi-nucleation dynamics of the two dimensional Potts model exhibits peculiar finite size effects, rather different from the ones arising in the phase-ordering of binary systems. In the latter, there are only two competing colours and the growth of the domains does not feel the finiteness of the system until some time $t_{\rm end}(L)$, when the domain sizes become comparable to L. At this point the coarsening process with a balanced competition among domains enters a final stage in which one domain eventually dominates and equilibrium is approached. For times $t \ll t_{\rm end}$ any (intensive) measurement does not depend on the value of L. In the Potts model, one observes an analogous behaviour when observing a quantity like R, as we discussed at the end of section 3. This L independence (for $t \ll t_{\rm end}(L)$) also holds true for the sizes $\mathcal{R}_1$ and $\mathcal{R}_2$ of the two prevailing colours. However, the number k of coarsening phases depends on L up to a value of L roughly as large as L_q, given in equation (15). Notice that this characteristic size diverges as $T \to T_{\rm c}$ for a given q as discussed above. Worst, the sizes $\mathcal{R}_n$ ($n \in [3, q]$) of the domains of the minority colours, do depend on L even if measured at times $t \ll t_{\rm end}$ (see figure 4). This different behaviour is perhaps at the origin of many controversies on the size dependence of the metastable dynamics.

One might wonder how it may be possible that the unrestricted quantity R (equation (5)) be size-independent whereas the restricted ones $\mathcal{R}_n$ do depend on L, given that R is representative of the average of the $\mathcal{R}_n$s (although the latter are obtained from the correlation function, see equation (13)). This occurs because R only fixes the average size of domains but not their colour, as it is schematically illustrated in figure 7. The configuration on the left shows a portion of a system of size $L_{\rm A}$ at a time t where six phases are present. On the right, instead, an analogous system with a different size $L_{\rm B} < L_{\rm A}$ is represented at the same time t. The represented portion of the first system equals the total size of the second. It can be seen that, although two phases (the green and the brown one) are absent in the smaller lattice (hence the number of colours is L dependent), the size of the domains does not change (hence is L independent).

J. Stat. Mech. (2022) 073204

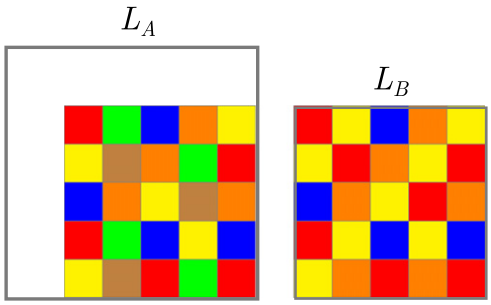

Figure 7. Two pictorial configurations of the bidimensional Potts model on the square lattice. The system on the right has a size $L_{\rm B}$ and the picture represents the whole lattice. The one on the left has a larger size $L_{\rm A} > L_{\rm B}$ but in the picture only a part of it, of size $L_{\rm B}$, is shown. The two systems are characterised by the same size of the domains, but in the right one the green and brown phases have disappeared.

5. Discussion

In this paper we studied the multi-nucleation phenomenon after a shallow quench of the Potts model with $4 < q \leqslant 100$ to $T \lesssim T_{\rm c}(q)$. A related study of the model with $q \gg 100$ addressing deep quenches to $T \ll T_{\rm c}(q)$ was presented in a companion article by some of us [35].

The main result of this paper, which is contained in equations (14)–(16), is that the number of nucleating phases of the two-dimensional Potts model with not too large q (see discussion below) increases logarithmically with the system size. (As the equation establishes, this growth is bounded by q itself.) The logarithmic behaviour informs us that this feature cannot be fully explained by the trivial geometrical fact that a larger system can *accommodate* a larger number of developing colours. If this were the origin, the snapshots in figure 2 should display an equal number of nucleating phases in portions with equal area of systems with different sizes. This, however, is not observed. For instance, comparing the systems of relative almost double size $L = 80$ (first line) and $L = 142$ (last row), at time $t = 80\,000$, one sees that there is only one nucleating colour (orange, besides a remnant of the disordered phase) in the smallest system, whereas there is typically more than one colour in a portion of area 80×80 of the system with $L = 142$.

This raises an important question which, by the way, concerns also the size dependence of the metastable state recalled in the introduction: how can a system with a very short coherence length (of the order of the nuclei size, as it can also be appreciated from the correlation function of figure 3) feel the system size logarithmically as in equation (16)?

The mechanism for ordering in systems with $q \gg 100$ is rather different from the one discussed here. In these systems after an extremely long waiting period (the longer the closer to $T_{\rm c}(q)$ at fixed q, or the larger q at $T/T_{\rm c}(q)$ fixed) the systems suddenly jump to a partially ordered blocked state with large domains. No 'sand' (disordered regions between clusters that can be seen in figure 2) lubricates the motion of the domain walls

J. Stat. Mech. (2022) 073204

in this case and the interfaces are mostly straight. Although the quench is to high T, even close to $T_c(q)$, these blocked states resemble the ones at zero temperature. We postpone the analysis of the ordering process under these $(q, T/T_c(q))$ conditions to a future publication. Still, an idea of the way in which the typical length scale R increases in time in this regime of parameters can be reached by looking at figures 6(c) and (d) in [35].

Acknowledgments

We thank A Vezzani for very useful comments, and F Chippari with whom two of us performed a parallel study of quenches towards parameters farther away from $T_c(q)$ [35]. We also wish to express out gratitude to H Van Beijeren who, as editor of this submission, made suggestions that helped us improve the quality of this manuscript.

References

[1] Debenedetti P G 1996 *Metastable Liquids* (Princeton, NJ: Princeton University Press)
[2] Rikvold P A and Gorman B M 1995 Recent results on the decay of metastable phases *Annual Reviews of Computational Physics I* ed D Stauffer (Singapore: World Scientific) ch 5 p 149
[3] Günther C C A, Rikvold P A and Novotny M A 1993 Numerical transfer-matrix study of metastability in the $d = 2$ Ising model *Phys. Rev. Lett.* **71** 3898
[4] Günther C C A, Rikvold P A and Novotny M A 1994 Application of a constrained-transfer-matrix method to metastability in the $d = 2$ Ising ferromagnet *Physica* A **212** 194
[5] Debenedetti P G and Stillinger F H 2001 Supercooled liquids and the glass transition *Nature* **410** 259
[6] Thirumalai D and Reddy G 2011 Are native proteins metastable? *Nat. Chem.* **3** 910
[7] Völker J, Klump H H and Breslauer K J 2008 DNA energy landscapes via calorimetric detection of microstate ensembles of metastable macrostates and triplet repeat diseases *Proc. Natl Acad. Sci. USA* **105** 18326
[8] Frenkel J 1946 *Kinetic Theory of Liquids* (Oxford: Oxford University Press)
[9] Laaksonen A, Talanquer V and Oxtoby D W 1995 Nucleation: measurements, theory, and atmospheric applications *Annu. Rev. Phys. Chem.* **46** 489
[10] Chaikin P M and Lubensky T C 1995 *Principles of Condensed Matter Physics* (Cambridge: Cambridge University Press)
[11] Becker R and Döring W 1935 Kinetische Behandlung der Keimbildung in übersättigten Dämpfen *Ann. Phys.* **416** 719
[12] Burton J J 1977 Nucleation theory *Statistical Mechanics, Part A: Equilibrium Techniques* ed B J Berne (New York: Plenum) p 195
[13] Penrose O and Lebowitz J L 1979 Towards a rigorous molecular theory of metastability *Studies in Statistical Mechanics VII: Fluctuation Phenomena* ed E Montroll and J L Lebowitz (Amsterdam: North-Holland) p 293
[14] Capocaccia D, Cassandro M and Olivieri E 1974 A study of metastability in the Ising model *Commun. Math. Phys.* **39** 185
[15] Penrose O and Lebowitz J L 1971 Rigorous treatment of metastable states in the van der Waals–Maxwell theory *J. Stat. Phys.* **3** 211
[16] Stillinger F H 1995 Statistical mechanics of metastable matter: superheated and stretched liquids *Phys. Rev.* E **52** 4685
[17] Corti D S and Debenedetti P G 1995 Metastability and constraints: a study of the superheated Leonard–Jones liquid in the void-constrained ensemble *Ind. Eng. Chem. Res.* **34** 3573
[18] Langer J S 1967 Theory of the condensation point *Ann. Phys., NY* **41** 108
[19] Langer J S 1968 Theory of nucleation rates *Phys. Rev. Lett.* **21** 973
[20] Langer J S 1980 *Systems Far from Equilibrium* (*Lecture Notes in Physics*) vol 132 ed L Garrido (Berlin: Springer) pp 12–47
[21] Gunther N J, Wallace D J and Nicole D A 1980 Goldstone modes in vacuum decay and first-order phase transitions *J. Phys. A: Math. Gen.* **13** 1755

J. Stat. Mech. (2022) 073204

[22] Schmitz F, Virnau P and Binder K 2013 Monte Carlo tests of nucleation concepts in the lattice gas model *Phys. Rev.* E **87** 053302
[23] Potts R B 1952 Some generalized order–disorder transformations *Math. Proc. Camb. Phil. Soc.* **48** 106
[24] Wu F Y 1982 The Potts model *Rev. Mod. Phys.* **54** 235
[25] Baxter R J 1982 *Exactly Solved Models in Statistical Mechanics* 1st edn (New York: Academic)
[26] Gunton J D, San Miguel M and Sahni P S 1983 *Phase Transitions and Critical Phenomena* vol 8 ed C Domb and J L Lebowitz (New York: Academic)
[27] Binder K 1987 Theory of first-order phase transitions *Rep. Prog. Phys.* **50** 783
[28] Oxtoby D W 1992 Homogeneous nucleation: theory and experiment *J. Phys.: Condens. Matter* **4** 7627
[29] Kelton K F and Greer A L 2010 *Nucleation in Condensed Matter* (Amsterdam: Elsevier)
[30] Meunier J L and Morel A 2000 Condensation and metastability in the 2D Potts model *Eur. Phys. J.* B **13** 341
[31] Loscar E S, Ferrero E E, Grigera T S and Cannas S A 2009 Nonequilibrium characterization of spinodal points using short time dynamics *J. Chem. Phys.* **131** 024120
[32] Ferrero E E, De Francesco J P, Wolovick N and Cannas S A 2011 q-state Potts model metastability study using optimized GPU-based Monte Carlo algorithms *Comput. Phys. Commun.* **183** 1578
[33] Ibáñez Berganza M, Coletti P and Petri A 2014 Anomalous metastability in a temperature-driven transition *Europhys. Lett.* **106** 56001
[34] Mazzarisi O, Corberi F, Cugliandolo L F and Picco M 2020 Metastability in the Potts model: exact results in the large q limit *J. Stat. Mech.* 063214
[35] Chippari F, Cugliandolo L F and Picco M 2021 Low-temperature universal dynamics of the bidimensional Potts model in the large q limit *J. Stat. Mech.* 093201
[36] Lifshitz I M 1962 *Zh. Éksp. Teor. Fiz.* **42** 1354 (Engl. transl. 1962 *Sov. Phys. JETP* **15** 939)
Lifshitz I M 1962 *Sov. Phys. – JETP* **15** 939 (Engl. transl.)
[37] Ferrero E E and Cannas S A 2007 Long-term ordering kinetics of the two-dimensional q-state Potts model *Phys. Rev.* E **76** 031108
[38] Olejarz J, Krapivsky P L and Redner S 2013 Zero-temperature coarsening in the 2D Potts model *J. Stat. Mech.* P06018
[39] Denholm J and Redner S 2019 Topology-controlled Potts coarsening *Phys. Rev.* E **99** 062142
[40] Denholm J 2021 High-degeneracy Potts coarsening *Phys. Rev.* E **103** 012119
[41] Glazier J A, Anderson M P and Grest G S 1990 Coarsening in the two-dimensional soap froth and the large-Q Potts model: a detailed comparison *Phil. Mag.* B **62** 615
[42] Sanders D P, Larralde H and Leyvraz F 2007 Competitive nucleation and the Ostwald rule in a generalized Potts model with multiple metastable phases *Phys. Rev.* B **75** 132101
[43] Ibáñez de Berganza M, Ferrero E E, Cannas S A, Loreto V and Petri A 2007 Phase separation of the Potts model in the square lattice *Eur. Phys. J. Spec. Top.* **143** 273
[44] Petri A, de Berganza M I and Loreto V 2008 Ordering dynamics in the presence of multiple phases *Phil. Mag.* **88** 3931
[45] Loureiro M P O, Arenzon J J and Cugliandolo L F 2010 Curvature-driven coarsening in the two-dimensional Potts model *Phys. Rev.* E **81** 021129
[46] Loureiro M P O, Arenzon J J and Cugliandolo L F 2012 Geometrical properties of the Potts model during the coarsening regime *Phys. Rev.* E **85** 021135
[47] Baxter R J 1973 Potts model at the critical temperature *J. Phys. C: Solid State Phys.* **6** L445
[48] Challa M S S, Landau D P and Binder K 1986 Finite-size effects at temperature-driven first-order transitions *Phys. Rev.* B **34** 1841
[49] Buffenoir E and Wallon S 1993 The correlation length of the Potts model at the first-order transition point *J. Phys. A: Math. Gen.* **26** 3045
[50] Corberi F, Cugliandolo L F, Esposito M and Picco M 2019 Multinucleation in the first-order phase transition of the 2D Potts model *J. Phys.: Conf. Ser.* **1226** 012009
[51] Corberi F, Lippiello E and Zannetti M 2006 Scaling and universality in the aging kinetics of the two-dimensional clock model *Phys. Rev.* E **74** 041106
[52] Wu F Y 1997 The infinite-state Potts model and restricted multidimensional partitions of an integer *Math. Comput. Modelling* **26** 269

J. Stat. Mech. (2022) 073204